Nonlinear Dyn (2015) 82:1691–1707
DOI 10.1007/s11071-015-2270-3

ORIGINAL PAPER

An improved time-delay saturation controller for suppression of nonlinear beam vibration

Jian Xu · Yueli Chen · Kwok Wai Chung

Received: 5 October 2014 / Accepted: 11 July 2015 / Published online: 25 July 2015

Abstract In this paper, a nonlinear saturation controller is improved by using quadratic velocity coupling term with time delay instead of the original quadratic position coupling term in the controller and adding a negative time-delay velocity feedback to the primary system. The improved controller is utilized to control the high-amplitude vibration of a flexible, geometrically nonlinear beam-like structure when the primary resonance and the 1:2 internal resonance occur simultaneously. To explain analytically mechanism of the saturation controlled system, an integral iterative method is presented to obtain the second-order approximations and the amplitude equations. It is shown that the quadratic velocity coupling term can enlarge the effective frequency bandwidth and enhance the performance of the vibration suppression by comparison with the quadratic position coupling term, and the linear velocity feedback can suppress the transient vibrations. The effects of different control parameters on saturation control are investigated. We found that time delays can be used as control parameters to change the effective frequency bandwidth and avoid the controller overload risk. The analyses show that numerical simulations are in good agreement with the analytical solutions.

Keywords Saturation controller · The integral iterative method · Quadratic velocity coupling term · Quadratic position coupling term · Time delay

J. Xu (✉) · Y. Chen
School of Aerospace Engineering and Applied Mechanics, Tongji University, Shanghai 200092, People's Republic of China
e-mail: xujian@tongji.edu.cn

Y. Chen
e-mail: chenyueli1986@126.com

K. W. Chung
Department of Mathematics, City University of Hong Kong, Kowloon, Hong Kong, People's Republic of China
e-mail: makchung@cityu.edu.hk

1 Introduction

If a system has quadratic nonlinearities, the saturation phenomenon occurs when its natural frequencies are in the ratio 1:2. The saturation control method based on the internal resonance and the saturation phenomenon is a novel one for vibration control. The applications of the saturation control method have attracted considerable attention in the past two decades, especially for the linear main system [1–7]. Recently, there have been more and more studies and applications of this method for the nonlinear main system. Li et al. [8] employed a saturation-based active absorber to suppress the high-amplitude vibration of a nonlinear plant subjected to principal external excitation. They found that the saturation control would have a wide suppression frequency bandwidth once the frequency of the absorber was appropriately tuned. El-Badawy, El-Deen [9] and Li et al. [10] applied a active nonlinear saturation-based controller to suppress the free vibration of a self-

excited plant. They demonstrated that the response of the plant could be independent of its parameters when the frequency of the absorber exactly equaled to half of the natural frequency of the plant. In [11], the saturation phenomenon and internal resonance is applied to suppress the steady-state and transient vibrations of helicopter rotor blade flapping. It is demonstrated that the saturation control is efficient in suppressing the steady-state vibrations. Warminski with his co-authors [12] used a nonlinear saturation controller to control the vibrations of a nonlinear beam subjected to self- and externally excitations. They found that the system might lose stabilities when the two type excitations interacted near the fundamental resonance zone. In Ref. [13], a nonlinear saturation controller was applied to control the undesired vibrations of a nonlinear magnetic levitation. They concluded that the natural frequency of the controller should be kept equal to one half of the excitation frequency in the control process.

The saturation control method is effective and robust near the resonance zone. However, the effective frequency bandwidth of the controller is too narrow and the transient vibrations are too long under the saturation control. To solve this problem, Pai and his coauthors [6] used quadratic velocity coupling term instead of quadratic position coupling term in the controller and added a negative velocity self-feedback to improve the original saturation controller.

Time delay can be used as an important control parameter. For example, it can change the range of the saturation control in [7] and can induces symmetry restoration in an asymmetric bistable system in [14]. Zhao and Xu [15] used the delayed feedback control and saturation control to suppress the vibration of a two degree-of-freedom dynamic vibration absorber system with a parametrically excited pendulum. In Ref. [16], Saeed and his co-authors concluded that time delay could avoid the saturation controller overload and generate chaotic motions.

In recent years, the vibration control of flexible beam systems has received much attentions [17–19]. In this paper, an improved saturation control method is used to control the transient and first mode steady-state vibrations of a flexible, geometrically nonlinear beam. Based on the saturation controller in [6], we improve the original saturation controller in [20] by using quadratic velocity coupling term with time delay instead of the original quadratic position coupling term in the controller and adding a negative time-delay velocity feedback to the primary system. We divide three cases to investigate the performance of the improved saturation controller, i.e., (1) keep the natural frequency of the saturation controller equal to one half of the natural frequency of the primary system ($\sigma_2 = 0$); (2) keep the natural frequency of the saturation controller equal to one half of the excitation frequency($\sigma_1 + \sigma_2 = 0$); (3) keep the excitation frequency equal to the natural frequency of the primary system($\sigma_1 = 0$). Effects of different control parameters on saturation control are studied for the above three cases. Finally, numerical simulations are presented to validate the analytical predictions.

2 Mathematical modeling

The governing equations describing the first mode vibrations of a nonlinear composite beam in Refs. [8,12,16,20,21] together with the saturation controller are in the following form

$$\begin{aligned} &\ddot{u} + 2\mu_1\omega_1\dot{u} + \omega_1^2 u + \alpha_1 u^3 - \beta(u\dot{u}^2 + u^2\ddot{u}) \\ &\quad = f\cos(\Omega t) + f_1 + f_2, \\ &\quad \ddot{v} + 2\mu_2\omega_2\dot{v} + \omega_2^2 v = f_3. \end{aligned} \tag{1}$$

where u denotes the response of the primary system, v denotes the response of the saturation controller, ω_1 is the natural frequency of the primary system, μ_1 is the damping ratio of the primary system, α_1 is the curvature nonlinearity coefficient, β denotes the inertia nonlinearity coefficient, μ_2 is the damping ratio of the controller, ω_2 is the natural frequency of the controller, f and Ω represent the forcing amplitude and frequency, respectively. There are two different feedback control strategies we consider in the following:

Feedback (1): $f_1 = 0$, $f_2 = \gamma v^2$, $f_3 = \alpha uv$, it is the original saturation controller in [20].

Feedback (2): $f_1 = -2\lambda\omega_1\dot{u}(t-\tau_1)$, $f_2 = \gamma v^2(t-\tau_2)$, $f_3 = \alpha\dot{u}(t-\tau_3)\dot{v}(t-\tau_3)$. We use $\alpha\dot{u}(t-\tau_3)\dot{v}(t-\tau_3)$ instead of αuv and add a negative velocity feedback $-2\lambda\omega_1\dot{u}(t-\tau_1)$ to increase the system damping, where τ_1, τ_2, τ_3 are time delays.

3 The integral iterative method

Vibrations of various kinds with time delay can be described by delay differential equations in the following form

$$\ddot{x}_i + \lambda_i x_i = \phi_i(x_i, \dot{x}_i, x_{i\tau}, \dot{x}_{i\tau}, x_j, \dot{x}_j, x_{j\tau}, \dot{x}_{j\tau}; \varepsilon_{p_i}, t) = \phi_i[t, \tau], \quad i, j = 1, 2, \cdots \tag{2}$$

where $x_{i\tau} = x_i(t-\tau)$ and ε_{p_i} is a parameter.

Theorem 1 *Every periodic solution of the differential equation* (2) *is a solution of the integro-differential equation*(see [22–24])

$$x_i(t) = \int_0^{2\pi} G_i[t, \sigma]\phi_i[\sigma, \tau]\,\mathrm{d}\sigma + \delta_{\lambda_i}^{n_i^2}(r_i \cos n_i t + s_i \sin n_i t), \tag{3}$$

and time delay terms can be transformed into

$$x_i(t-\tau) = \int_0^{2\pi} G_i[t-\tau, \sigma]\phi_i[\sigma, \tau]\,\mathrm{d}\sigma + \delta_{\lambda_i}^{n_i^2}(r_i \cos n_i(t-\tau) + s_i \sin n_i(t-\tau)), \tag{4}$$

where $G_i[t, \sigma] = \frac{1}{\pi}\left(\frac{1}{2\lambda_i} + \sum_{j=1}^{\infty} \frac{\cos j(t-\sigma)}{\vartheta\lambda_i - j^2}\right)$, $G_i[t-\tau, \sigma] = \frac{1}{\pi}\left(\frac{1}{2\lambda_i} + \sum_{j=1}^{\infty} \frac{\cos j\tau \cos j(t-\sigma) + \sin j\tau \sin j(t-\sigma)}{\vartheta\lambda_i - j^2}\right)$ *are the corresponding generalized Green's functions, where*

$$\delta_{\lambda_i}^{n_i^2} = \begin{cases} 1 & \lambda_i = n_i^2, n_i \quad \textit{being an integer}, \\ 0 & \textit{otherwise}, \end{cases}$$

is the Kronecker symbol, and $\vartheta = \vartheta_{\lambda_i}^{n_i^2} = 1 - \delta_{\lambda_i}^{n_i^2}$.

If $\lambda_i = n_i^2$ (n_i *being an integer for the resonance case), the parameters* r_i, s_i *can be determined by the periodicity equations* (see [22–24])

$$r_i = \frac{1}{\pi}\int_0^{2\pi} x_i(t)\cos n_i t\,\mathrm{d}t, \qquad s_i = \frac{1}{\pi}\int_0^{2\pi} x_i(t)\sin n_i t\,\mathrm{d}t, \tag{5}$$

which are equivalent to

$$\int_0^{2\pi} \phi_i[t, \tau]\cos n_i t\,\mathrm{d}t = \int_0^{2\pi} \phi_i[t, \tau]\sin n_i t\,\mathrm{d}t = 0. \tag{6}$$

The solutions of (3) and (4) can be obtained by successive approximations of $x_{ik}(t)$, $x_{ik}(t-\tau)$, $k = 1, 2, 3, \ldots$, which are given by

$$x_{ik}(t) = \int_0^{2\pi} G_i[t, \sigma]\phi_{i,k-1}[\sigma, \tau]\,\mathrm{d}\sigma + \delta_{\lambda_i}^{n_i^2}(r_i \cos(n_i t) + s_i \sin(n_i t)), \tag{7}$$

$$x_{ik}(t-\tau) = \int_0^{2\pi} G_i[t-\tau, \sigma]\phi_{i,k-1}[\sigma, \tau]\,\mathrm{d}\sigma + \delta_{\lambda_i}^{n_i^2}(r_i \cos n_i(t-\tau) + s_i \sin n_i(t-\tau)), \tag{8}$$

where

$$\phi_{i0}[t, \tau] = \begin{cases} 0, & \lambda_i = n_i^2 \\ \phi[0,0,0,0,0,0,0,0; \varepsilon_{p_i}, t] & \lambda_i \neq n_i^2 \end{cases}$$

$$\phi_{ik}[t, \tau] = \phi_i[x_{ik}(t), \dot{x}_{ik}(t), x_{ik}(t-\tau), \dot{x}_{ik}(t-\tau), x_{jk}(t), \dot{x}_{jk}(t), x_{jk}(t-\tau), \dot{x}_{jk}(t-\tau); \varepsilon_{p_i}, t] \quad k = 1, 2, 3, \cdots \tag{9}$$

The integral equation method was introduced by G. Schmidt [22]. In our previous works [23,24], we utilized this method to deal with delay differential equations and demonstrated that the accuracy was remarkable. However, the expressions of this method is not rigorous when dealing with delay differential equations. In this section, we improve the integral equation method by adding the Eq. (4) and rewriting the successive program. Now, we rename this improved method as the integral iterative method because of more iterative processes.

4 Amplitude equations

From the previously published works [1–13,15,16,20], it is concluded that the saturation phenomenon occurs when the primary resonance and the 1:2 internal resonance occur simultaneously. To analyze the saturation control, two detuning parameters σ_1, σ_2 are introduced as follows

$$\Omega = \omega_1 + \sigma_1, \quad \omega_1 = 2\omega_2 + \sigma_2. \tag{10}$$

We introduce a dimensionless time again by

$$t_1 = \frac{1}{2}\Omega t, \quad \tau_1 = \frac{1}{2}\Omega\tau, \tag{11}$$

Here, for simplicity, we still replace t_1, τ_1 by t, τ.

For the Feedback (2) controlled system, the Eq. (1) can be transformed into the following form:

$$\ddot{u} + 4u = \frac{4}{\Omega^2}\Big[(2\Omega\sigma_1 - \sigma_1^2)u - \mu_1\omega_1\Omega\dot{u} - \alpha_1 u^3 + \frac{1}{4}\Omega^2\beta(u\dot{u}^2 + u^2\ddot{u}) + f\cos(2t) + \gamma v^2(t-\tau_2) - \lambda\omega_1\Omega\dot{u}(t-\tau_1)\Big],$$

$$\ddot{v}+v=\frac{4}{\Omega^2}\left[\left(\frac{1}{2}\Omega(\sigma_1+\sigma_2)-\frac{1}{4}(\sigma_1+\sigma_2)^2\right)v+\frac{1}{4}\Omega^2\alpha\dot{u}(t-\tau_3)\dot{v}(t-\tau_3)-\mu_2\omega_2\Omega\dot{v}\right]. \tag{12}$$

For the Eq. (12), the corresponding generalized Green's functions are

$$\lambda_1=4,$$

$$G_1[t,\sigma]=\frac{1}{\pi}\left[\frac{1}{8}+\frac{1}{3}\cos(t-\sigma)-\frac{1}{4}\cos(2(t-\sigma))+\sum_{j=3}^{\infty}\frac{\cos(j(t-\sigma))}{4-j^2}\right], \tag{13}$$

$$G_1[t-\tau,\sigma]=\frac{1}{\pi}\left[\frac{1}{8}+\frac{1}{3}\cos(t-\tau-\sigma)-\frac{1}{4}\cos 2(t-\tau-\sigma)+\sum_{j=3}^{\infty}\frac{\cos j(t-\tau-\sigma)}{4-j^2}\right], \tag{14}$$

$$\lambda_2=1,$$

$$G_2[t,\sigma]=\frac{1}{\pi}\left[\frac{1}{2}-\cos(t-\sigma)+\sum_{j=2}^{\infty}\frac{\cos j(t-\sigma)}{1-j^2}\right], \tag{15}$$

$$G_2[t-\tau,\sigma]=\frac{1}{\pi}\left[\frac{1}{2}-\cos(t-\tau-\sigma)+\sum_{j=2}^{\infty}\frac{\cos j(t-\tau-\sigma)}{1-j^2}\right]. \tag{16}$$

From Eqs. (7) and (8), we have the first approximation in the following form

$$u_1(t)=r_1\cos(2t)+s_1\sin(2t), \tag{17}$$

$$v_1(t)=r_2\cos t+s_2\sin t, \tag{18}$$

$$u_1(t-\tau_i)=r_1\cos(2t-2\tau_i)+s_1\sin(2t-2\tau_i), \tag{19}$$

$$v_1(t-\tau_i)=r_2\cos(t-\tau_i)+s_2\sin(t-\tau_i), \tag{20}$$

$i=1,2,3,\ldots.$

Substituting Eqs. (17)–(20) into Eqs. (7) and (8), we obtain the second approximations in the form

$$\begin{aligned}u_2(t)=&\int_0^{2\pi}\frac{1}{\pi}\left[\frac{1}{8}+\frac{1}{3}\cos(t-\sigma)-\frac{1}{4}\cos 2(t-\sigma)+\sum_{j=3}^{\infty}\frac{\cos j(t-\sigma)}{4-j^2}\right]\frac{4}{\Omega^2}[(2\Omega\sigma_1-\sigma_1^2)u_1(\sigma)\\&-\mu_1\omega_1\Omega\dot{u}_1(\sigma)-\alpha_1u_1^3(\sigma)+\frac{1}{4}\Omega^2\beta(u_1(\sigma)\dot{u}_1^2(\sigma)+u_1^2(\sigma)\ddot{u}_1(\sigma))+f\cos(2\sigma)+\gamma v_1^2(\sigma-\tau_2)\\&-\lambda\omega_1\Omega\dot{u}_1(\sigma-\tau_1)]\,d\sigma+r_1\cos(2t)+s_1\sin(2t)\\=&\frac{r_2^2\gamma}{2\Omega^2}+\frac{s_2^2\gamma}{2\Omega^2}+\left(\frac{r_1^3\beta}{16}-\frac{3}{16}r_1s_1^2\beta+\frac{r_1^3\alpha_1}{32\Omega^2}-\frac{3r_1s_1^2\alpha_1}{32\Omega^2}\right)\cos(6t)+\left(\frac{3}{16}r_1^2s_1\beta-\frac{s_1^3\beta}{16}+\frac{3r_1^2s_1\alpha_1}{32\Omega^2}-\frac{s_1^3\alpha_1}{32\Omega^2}\right)\sin(6t)\\&+\left(r_1+\frac{r_1^3\beta}{2}+\frac{1}{2}r_1s_1^2\beta-\frac{f}{\Omega^2}+\frac{3r_1^3\alpha_1}{4\Omega^2}+\frac{3r_1s_1^2\alpha_1}{4\Omega^2}+\frac{r_1\sigma_1^2}{\Omega^2}-\frac{2r_1\sigma_1}{\Omega}+\frac{2s_1\mu_1\omega_1}{\Omega}+\frac{2s_1\lambda\omega_1\cos(2\tau_1)}{\Omega}-\frac{r_2^2\gamma\cos(2\tau_2)}{2\Omega^2}+\frac{s_2^2\gamma\cos(2\tau_2)}{2\Omega^2}+\frac{2r_1\lambda\omega_1\sin(2\tau_1)}{\Omega}+\frac{r_2s_2\gamma\sin(2\tau_2)}{\Omega^2}\right)\cos(2t)\\&+\left(s_1+\frac{1}{2}r_1^2s_1\beta+\frac{s_1^3\beta}{2}+\frac{3r_1^2s_1\alpha_1}{4\Omega^2}+\frac{3s_1^3\alpha_1}{4\Omega^2}+\frac{s_1\sigma_1^2}{\Omega^2}-\frac{2s_1\sigma_1}{\Omega}-\frac{2r_1\mu_1\omega_1}{\Omega}-\frac{2r_1\lambda\omega_1\cos(2\tau_1)}{\Omega}-\frac{r_2s_2\gamma\cos(2\tau_2)}{2\Omega^2}+\frac{2s_1\lambda\omega_1\sin(2\tau_1)}{\Omega}-\frac{r_2^2\gamma\sin(2\tau_2)}{2\Omega^2}+\frac{s_2^2\gamma\sin(2\tau_2)}{2\Omega^2}\right)\sin(2t),\end{aligned} \tag{21}$$

$$\begin{aligned}v_2(t)=&\int_0^{\pi}\frac{1}{2\pi}\left[\frac{1}{2}-\cos(t-\sigma)+\sum_{j=2}^{\infty}\frac{\cos j(t-\sigma)}{1-j^2}\right]\frac{4}{\Omega^2}\left[\left(\frac{1}{2}\Omega(\sigma_1+\sigma_2)-\frac{1}{4}(\sigma_1+\sigma_2)^2\right)v_1(\sigma)-\mu_2\omega_2\Omega\dot{v}_1(\sigma)+\frac{1}{4}\Omega^2\alpha\dot{u}_1(\sigma-\tau_3)\dot{v}_1(\sigma-\tau_3)\right]d\sigma\\&+r_2\cos t+s_2\sin t\\=&\cos t\left(r_2+\frac{r_2\sigma_1^2}{\Omega^2}+\frac{2r_2\sigma_1\sigma_2}{\Omega^2}-\frac{2r_2\sigma_2}{\Omega}+\frac{4s_2\mu_2\omega_2}{\Omega}-r_1r_2\alpha\cos\tau_3+\frac{r_2\sigma_2^2}{\Omega^2}-\frac{2r_2\sigma_1}{\Omega}-s_1s_2\alpha\cos\tau_3+r_2s_1\alpha\sin\tau_3-r_1s_2\alpha\sin\tau_3\right)+\sin t\left(s_2+\frac{s_2\sigma_1^2}{\Omega^2}+\frac{2s_2\sigma_1\sigma_2}{\Omega^2}+\frac{s_2\sigma_2^2}{\Omega^2}-\frac{2s_2\sigma_1}{\Omega}-\frac{2s_2\sigma_2}{\Omega}-\frac{4r_2\mu_2\omega_2}{\Omega}-r_2s_1\alpha\cos\tau_3+r_1s_2\alpha\cos\tau_3-r_1r_2\alpha\sin\tau_3-s_1s_2\alpha\sin\tau_3\right)+\cos(3t)\left(\frac{1}{8}r_1r_2\alpha\cos(3\tau_3)-,\frac{1}{8}s_1s_2\alpha\cos(3\tau_3)-\frac{1}{8}r_2s_1\alpha\sin(3\tau_3)-\frac{1}{8}r_1s_2\alpha\sin(3\tau_3)\right)+\sin(3t)\left(\frac{1}{8}r_2s_1\alpha\cos(3\tau_3)\right.\end{aligned}$$

$$+\frac{1}{8}r_1s_2\alpha\cos(3\tau_3)+\frac{1}{8}r_1r_2\alpha\sin(3\tau_3)-\frac{1}{8}s_1s_2\alpha\sin(3\tau_3)\Big). \quad (22)$$

Substituting Eqs. (21) and (22) into the solvability conditions (5) yields

$$\frac{r_1^3\beta}{2}+\frac{1}{2}r_1s_1^2\beta-\frac{f}{\Omega^2}+\frac{3r_1^3\alpha_1}{4\Omega^2}+\frac{3r_1s_1^2\alpha_1}{4\Omega^2}+\frac{r_1\sigma_1^2}{\Omega^2}-\frac{2r_1\sigma_1}{\Omega}+\frac{2s_1\mu_1\omega_1}{\Omega}+\frac{2s_1\lambda\omega_1\cos(\Omega\tau_1)}{\Omega}-\frac{r_2^2\gamma\cos(\Omega\tau_2)}{2\Omega^2}+\frac{s_2^2\gamma\cos(\Omega\tau_2)}{2\Omega^2}+\frac{2r_1\lambda\omega_1\sin(\Omega\tau_1)}{\Omega}+\frac{r_2s_2\gamma\sin(\Omega\tau_2)}{\Omega^2}=0, \quad (23)$$

$$\frac{s_1^3\beta}{2}+\frac{1}{2}s_1r_1^2\beta+\frac{3s_1^3\alpha_1}{4\Omega^2}+\frac{3s_1r_1^2\alpha_1}{4\Omega^2}+\frac{s_1\sigma_1^2}{\Omega^2}-\frac{2s_1\sigma_1}{\Omega}-\frac{2r_1\lambda\omega_1\cos(\Omega\tau_1)}{\Omega}-\frac{r_2^2\gamma\sin(\Omega\tau_2)}{2\Omega^2}-\frac{2r_1\mu_1\omega_1}{\Omega}+\frac{s_2^2\gamma\sin(\Omega\tau_2)}{2\Omega^2}+\frac{2s_1\lambda\omega_1\sin(\Omega\tau_1)}{\Omega}-\frac{r_2s_2\gamma\cos(\Omega\tau_2)}{\Omega^2}=0, \quad (24)$$

$$\frac{r_2\sigma_1^2}{\Omega^2}+\frac{2r_2\sigma_1\sigma_2}{\Omega^2}+\frac{r_2\sigma_2^2}{\Omega^2}-\frac{2r_2\sigma_1}{\Omega}-\frac{2r_2\sigma_2}{\Omega}+\frac{4s_2\mu_2\omega_2}{\Omega}-r_1r_2\alpha\cos\left(\frac{\Omega\tau_3}{2}\right)-s_1s_2\alpha\cos\left(\frac{\Omega\tau_3}{2}\right)+r_2s_1\alpha\sin\left(\frac{\Omega\tau_3}{2}\right)-r_1s_2\alpha\sin\left(\frac{\Omega\tau_3}{2}\right)=0, \quad (25)$$

$$\frac{s_2\sigma_1^2}{\Omega^2}+\frac{2s_1\sigma_1\sigma_2}{\Omega^2}+\frac{s_2\sigma_2^2}{\Omega^2}-\frac{2s_2\sigma_1}{\Omega}-\frac{2s_2\sigma_2}{\Omega}-\frac{4r_2\mu_2\omega_2}{\Omega}-r_1r_2\alpha\sin\left(\frac{\Omega\tau_3}{2}\right)-s_1s_2\alpha\sin\left(\frac{\Omega\tau_3}{2}\right)-r_2s_1\alpha\cos\left(\frac{\Omega\tau_3}{2}\right)+r_1s_2\alpha\cos\left(\frac{\Omega\tau_3}{2}\right)=0. \quad (26)$$

For convenience to analyze the dynamics of the original equation (1), we denote the amplitude of the primary system $A_1=\sqrt{r_1^2+s_1^2}$ and the amplitude of the controller $A_2=\sqrt{r_2^2+s_2^2}$. To simplify the above four amplitude equations (23)–(26), we transform them into the form of the Cartesian coordinates given by

$$(8A_1\mu_1\Omega\omega_1+8A_1\lambda\Omega\omega_1\cos(\Omega\tau_1))\sin\theta_1+(3A_1^3\alpha_1+4A_1\sigma_1^2-8A_1\sigma_1\Omega+8A_1\lambda\Omega\omega_1\sin(\Omega\tau_1)+2A_1^3\beta\Omega^2)\cos\theta_1-4f-2A_2^2\gamma\cos(2\theta_2+\Omega\tau_2)=0, \quad (27)$$

$$(-8A_1\mu_1\Omega\omega_1-8A_1\lambda\Omega\omega_1\cos(\Omega\tau_1))\cos\theta_1+(3A_1^3\alpha+4A_1\sigma_1^2-8A_1\sigma_1\Omega+8A_1\lambda\Omega\omega_1\sin(\Omega\tau_1)+2A_1^3\beta\Omega^2)\sin\theta_1-2A_2^2\gamma\sin(2\theta_2+\Omega\tau_2)=0, \quad (28)$$

$$(A_2\sigma_1^2+2A_2\sigma_1\sigma_2+A_2\sigma_2^2-2A_2\sigma_1\Omega-2A_2\sigma_2\Omega)\cos\theta_2-A_1A_2\alpha\Omega^2\cos\left(\theta_1-\theta_2+\frac{1}{2}\Omega\tau_3\right)+4A_2\mu_2\Omega\omega_2\sin\theta_2=0, \quad (29)$$

$$(A_2\sigma_1^2+2A_2\sigma_1\sigma_2+A_2\sigma_2^2-2A_2\sigma_1\Omega-2A_2\sigma_2\Omega)\sin\theta_2-A_1A_2\alpha\Omega^2\sin\left(\theta_1-\theta_2+\frac{\Omega\tau_3}{2}\right)-4A_2\mu_2\Omega\omega_2\cos\theta_2=0. \quad (30)$$

where $r_1=A_1\cos\theta_1$, $s_1=A_1\sin\theta_1$, $r_2=A_2\cos\theta_2$, $s_2=A_2\sin\theta_2$. To simplify Eqs. (27)–(30), we make some simple calculations in the following:

Eq. (27)$\times\cos\theta_1+$ Eq. (28) $\times\sin\theta_1$ is

$$4f\cos\theta_1+2A_2^2\gamma\cos(\theta_1-2\theta_2-\Omega\tau_2)=A_1(4\sigma_1^2-8\Omega\sigma_1+A_1^2(3\alpha_1+2\beta\Omega^2)+8\lambda\Omega\omega_1\sin(\Omega\tau_1))=0. \quad (31)$$

Eq. (27) $\times\sin\theta_1-$ Eq. (28) $\times\cos\theta_1$ is

$$8A_1\Omega\omega_1(\mu_1+\lambda\cos(\Omega\tau_1))=4f\sin\theta_1+2A_2^2\gamma\sin(\theta_1-2\theta_2-\Omega\tau_2). \quad (32)$$

Eq. (29) $\times\sin\theta_2-$ Eq. (30) $\times\cos\theta_2$ is

$$A_2\Omega(4\mu_2\omega_2+A_1\alpha\Omega\sin(\theta_1-2\theta_2+\frac{\Omega\tau_3}{2}))=0. \quad (33)$$

Eq. (29) $\times\cos\theta_2+$ Eq. (30) $\times\sin\theta_2$ is

$$A_2\left((\sigma_1+\sigma_2)(\sigma_1+\sigma_2-2\Omega)-A_1\alpha\Omega^2\cos\left(\theta_1-2\theta_2+\frac{\Omega\tau_3}{2}\right)\right)=0. \quad (34)$$

Solving Eq. (31)–(34) and eliminating $\cos\theta_1$, $\sin\theta_1$, $\cos(\theta_1-2\theta_2)$, $\sin(\theta_1-2\theta_2)$ by means of the relations $\cos\theta_1^2+\sin\theta_1^2=1$, $\cos(\theta_1-2\theta_2)^2+\sin(\theta_1-2\theta_2)^2=1$ yield the amplitude equations for two possible cases.

Case 1 The controller does not activate, i.e., $A_1\neq 0$, $A_2=0$, we have the amplitude equation on A_1 from (31) and (32)

$$16f^2=A_1^2(64\Omega^2\omega_1^2(\mu_1+\lambda\cos(\Omega\tau_1))^2+(4\sigma_1(\sigma_1-2\Omega)+A_1^2(3\alpha_1+2\beta\Omega^2)+8\lambda\Omega\omega_1\sin(\Omega\tau_1))^2). \quad (35)$$

Case 2 The controller activates, i.e., $A_1 \neq 0,\ A_2 \neq 0$, then we have the amplitude equations from (31)–(34) in the following form

$$(\sigma_1+\sigma_2)^2(\sigma_1+\sigma_2-2\Omega)^2 + 16\mu_2^2\Omega^2\omega_2^2 = A_1^2\alpha^2\Omega^4, \tag{36}$$

$$\begin{aligned}
&16f^2A_1^2\alpha^2\Omega^4\\
&=\Big[A_1^2\alpha\Omega^2(4\sigma_1(\sigma_1-2\Omega)+A_1^2(3\alpha_1+2\beta\Omega^2)\\
&\quad+8\lambda\Omega\omega_1\sin(\Omega\tau_1))-4\mu_2\Omega\omega_2\sin\left(\frac{1}{2}(2\tau_2+\tau_3)\Omega\right)\\
&\quad-2A_2^2\gamma\left((\sigma_1+\sigma_2)(\sigma_1+\sigma_2-2\Omega)\cos\left(\frac{1}{2}(2\tau_2+\tau_3)\Omega\right)\right)\Big]^2\\
&\quad+\Big[8A_1^2\alpha\Omega^3\omega_1(\mu_1+\lambda\cos(\Omega\tau_1))\\
&\quad+2A_2^2\gamma\left(4\mu_2\Omega\omega_2\cos\left(\frac{1}{2}(2\tau_2+\tau_3)\Omega\right)\right.\\
&\quad\left.+(\sigma_1+\sigma_2)(\sigma_1+\sigma_2-2\Omega)\sin\left(\frac{1}{2}(2\tau_2+\tau_3)\Omega\right)\right)\Big]^2.
\end{aligned} \tag{37}$$

For the Feedback (1) controlled system, the amplitude equations can be obtained in the above similar process.

Case 1 The controller does not activate, i.e., $A_1 \neq 0,\ A_2 = 0$

$$\begin{aligned}
&(8A_1\mu_1\Omega\omega_1)^2+[4A_1\sigma_1^2+A_1^3(3\alpha_1+2\beta\Omega^2)\\
&-8A_1\sigma_1\Omega]^2=16f^2.
\end{aligned} \tag{38}$$

Case 2 The controller activates, i.e., $A_1 \neq 0,\ A_2 \neq 0$

$$(\sigma_1+\sigma_2)^2(\sigma_1+\sigma_2-2\Omega)^2 + 16\mu_2^2\Omega^2\omega_2^2 = 4A_1^2\alpha^2, \tag{39}$$

$$\begin{aligned}
&16[2A_1^2\alpha\mu_1\Omega\omega_1+A_2^2\gamma\mu_2\Omega\omega_2]^2\\
&+[3A_1^4\alpha\alpha_1+4A_1^2\alpha\sigma_1^2-A_2^2\gamma\sigma_1^2-2A_2^2\gamma\sigma_1\sigma_2\\
&-A_2^2\gamma\sigma_2^2-8A_1^2\alpha\sigma_1+2A_2^2\gamma\Omega(\sigma_1+\sigma_2)\Omega\\
&+2A_1^4\alpha\beta\Omega^2]^2=16A_1^2f^2\alpha^2.
\end{aligned} \tag{40}$$

5 Stability of periodic solutions

To study the stability of the periodic solutions of Eq. (1), we first perturb the periodic solution $u = u_2(t) = \frac{(r_2^2+s_2^2)\gamma}{2\Omega^2}+r_1\cos 2t+s_1\sin 2t$, $v = v_2(t) = r_2\cos t + s_2\sin t$ (omit the higher order terms in Eqs. (21) and (22) because of the weak nonlinearities) by introducing disturbance terms $z_1(t), z_2(t)$. Replacing $u_2(t), v_2(t)$ by $u_2(t)+z_1(t)$, $v_2(t)+z_2(t)$ in Eq. (12) and linearizing in $z_1(t)$, $z_2(t)$, we obtain

$$\begin{aligned}
\ddot{z}_1+4z_1 &= \frac{4}{\Omega^2}\Big[\left(2\Omega\sigma_1-\sigma_1^2\right)z_1-\mu_1\omega_1\Omega\dot{z}_1-3\alpha_1u_2^2z_1\\
&\quad+\frac{1}{4}\Omega^2\beta(\dot{u}_2z_1+2u_2\dot{u}_2\dot{z}_1+2u_2\ddot{u}_2z_1+u_2^2\ddot{z}_1)\\
&\quad+2\gamma v_2(t-\tau_2)z_2(t-\tau_2)-\lambda\omega_1\Omega\dot{z}_1(t-\tau_1)\Big],
\end{aligned} \tag{41}$$

$$\begin{aligned}
\ddot{z}_2+z_2 &= \frac{4}{\Omega^2}\left[\left(\frac{1}{2}\Omega(\sigma_1+\sigma_2)-\frac{1}{4}(\sigma_1+\sigma_2)^2\right)z_2\right.\\
&\quad-\mu_2\omega_2\Omega\dot{z}_2+\frac{1}{4}\Omega^2\alpha\dot{v}_2(t-\tau_3)\dot{z}_1(t-\tau_3)\\
&\quad\left.+\frac{1}{4}\Omega^2\alpha\dot{u}_2(t-\tau_3)\dot{z}_2(t-\tau_3)\right].
\end{aligned}$$

For convenience to investigate the stability of the periodic solutions, the nonlinear terms in Eq. (41) are written as

$$\begin{aligned}
\phi_1(t) &= u_2^2(t)\\
&= a_0+a_1\cos 2t+a_2\sin 2t+a_3\cos 4t\\
&\quad+a_4\sin 4t;\\
\phi_2(t) &= \dot{u}_2^2(t)\\
&= b_0+b_1\cos 4t+b_2\sin 4t;\\
\phi_3(t) &= u_2(t)\ddot{u}_2(t)\\
&= c_0+c_1\cos 2t+c_2\sin 2t+c_3\cos 4t\\
&\quad+c_4\sin 4t;\\
\phi_4(t) &= u_2(t)\dot{u}_2(t)\\
&= d_1\cos(2t)+d_2\sin(2t)+d_3\cos(4t)\\
&\quad+d_4\sin(4t);
\end{aligned}$$

where

$$\begin{aligned}
a_0 &= \frac{r_1^2}{2}+\frac{s_1^2}{2}+\frac{r_2^4\gamma^2}{4\Omega^4}+\frac{r_2^2s_2^2\gamma^2}{2\Omega^4}+\frac{s_2^4\gamma^2}{4\Omega^2},\\
a_1 &= \frac{r_1r_2^2\gamma}{\Omega^2}+\frac{r_1s_2^2\gamma}{\Omega^2},\quad a_2=\frac{r_2^2s_1\gamma}{\Omega^2}+\frac{s_1s_2^2\gamma}{\Omega^2},\\
a_3 &= \frac{r_1^2}{2}-\frac{s_1^2}{2},\quad a_4=r_1s_1,\quad b_0=2r_1^2+2s_1^2,\\
b_1 &= -2r_1^2+2s_1^2,\quad b_2=-4r_1s_1,\\
c_0 &= -2r_1^2-2s_1^2,\quad c_1=-\frac{2r_1r_2^2\gamma}{\Omega^2}-\frac{2r_1s_2^2\gamma}{\Omega^2},\\
c_2 &= -\frac{2r_2^2s_1\gamma}{\Omega^2}-\frac{2s_1s_2^2\gamma}{\Omega^2},\quad c_3=-2r_1^2+2s_1^2,\\
c_4 &= -4r_1s_1,\quad d_1=\frac{r_2^2s_1\gamma}{\Omega^2}+\frac{s_1s_2^2\gamma}{\Omega^2},
\end{aligned}$$

$$d_2 = -\frac{r_1 r_2^2 \gamma}{\Omega^2} - \frac{r_1 s_2^2 \gamma}{\Omega^2},$$
$$d_3 = 2r_1 s_1, \quad d_4 = -r_1^2 + s_1^2.$$

Eq. (41) change into

$$\begin{aligned}\ddot{z}_1 + 4z_1 = \frac{4}{\Omega^2}\Big[&(2\Omega\sigma_1 - \sigma_1^2)z_1 - \mu_1\omega_1\Omega\dot{z}_1 \\ &- 3\alpha_1\phi_1(t)z_1 + \frac{1}{4}\Omega^2\beta(\phi_2(t)z_1 + 2\phi_4(t)\dot{z}_1 \\ &+ 2\phi_3(t)z_1 + \phi_1(t)\ddot{z}_1) + 2\gamma v_2(t-\tau_2) \\ &\times z_2(t-\tau_2) - \lambda\omega_1\Omega\dot{z}_1(t-\tau_1)\Big], \qquad (42)\end{aligned}$$

$$\begin{aligned}\ddot{z}_2 + z_2 = \frac{4}{\Omega^2}\Big[&\left(\frac{1}{2}\Omega(\sigma_1+\sigma_2) - \frac{1}{4}(\sigma_1+\sigma_2)^2\right)z_2 \\ &+ \frac{1}{4}\Omega^2\alpha\dot{v}_2(t-\tau_3)\dot{z}_1(t-\tau_3) - \mu_2\omega_2\Omega\dot{z}_2 \\ &+ \frac{1}{4}\Omega^2\alpha\dot{u}_2(t-\tau_3)\dot{z}_2(t-\tau_3)\Big].\end{aligned}$$

Corresponding to the Floquet theory, the solution of Eq. (42) can be written as

$$z_i(t) = \exp(\rho t)Z_i(t), \quad i = 1,\ 2. \qquad (43)$$

The above Eqs. (42) change into

$$\begin{aligned}\ddot{Z}_1 + 4Z_1 = &\Big(b_0\beta + 2c_0\beta - \rho^2 + a_0\beta\rho^2 - \frac{12a_0\alpha_1}{\Omega^2} \\ &- \frac{4\sigma_1^2}{\Omega^2} + \frac{8\sigma_1}{\Omega} - \frac{4\mu_1\rho\omega_1}{\Omega} + \frac{1}{\Omega^2}(2\beta(c_1+d_1\rho)\Omega^2 \\ &+ a_1(\beta\rho^2\Omega^2 - 12\alpha_1)\Big)\cos(2t) + \frac{1}{\Omega^2}(\beta(b_1 \\ &+ 2(c_3+d_3\rho))\Omega^2 + a_3(\beta\rho^2\Omega^2 - 12\alpha_1))\cos(4t) \\ &+ \frac{1}{\Omega^2}\left(2\beta(c_2+d_2\rho)\Omega^2 + a_2(\beta\rho^2\Omega^2 - 12\alpha_1)\right)\sin(2t) \\ &+ \frac{1}{\Omega^2}(\beta(b_2 + 2(c_4+d_4\rho))\Omega^2 + a_4(\beta\rho^2\Omega^2 \\ &- 12\alpha_1))\sin(4t))\,Z_1(t) - \frac{4\exp(-\rho\tau_1)\lambda\rho\omega_1 Z_1(t-\tau_1)}{\Omega} \\ &+ \Big(\frac{8\exp(-\rho\tau_2)r_2\gamma\cos(t-\tau_2)}{\Omega^2} \\ &+ \frac{8\exp(-\rho\tau_2)s_2\gamma\sin(t-\tau_2)}{\Omega^2}\Big)Z_2(t-\tau_2) + (-2\rho \\ &+ 2a_0\beta\rho - \frac{4\mu_1\omega_1}{\Omega} + 2\beta(d_1 + a_1\rho)\cos(2t) + 2\beta(d_3 \\ &+ a_3\rho)\cos(4t) + 2\beta(d_2 + a_2\rho)\sin(2t) + 2\beta(d_4 \\ &+ a_4\rho)\sin(4t))\dot{Z}_1(t) + (a_0\beta + a_1\beta\cos(2t) \\ &+ a_3\beta\cos(4t) + a_2\beta\sin(2t) + a_4\beta\sin(4t))\ddot{Z}_1(t) \\ &- \frac{4\exp(-\rho\tau_1)\lambda\omega_1\dot{Z}_1(t-\tau_1)}{\Omega}, \qquad (44)\end{aligned}$$

$$\begin{aligned}\ddot{Z}_2 + Z_2 = &\exp(-\rho\tau_3)\alpha\rho(s_2\cos(t-\tau_3) \\ &- r_2\sin(t-\tau_3))Z_1(t-\tau_3) + \Big(-\rho^2 - \frac{(\sigma_1+\sigma_2)^2}{\Omega^2} \\ &+ \frac{2(\sigma_1+\sigma_2)}{\Omega} - \frac{4\mu_2\rho\omega_2}{\Omega}\Big)Z_2 \\ &+ 2\exp(-\rho\tau_3)\alpha\rho(s_1\cos(2(t-\tau_3)) \\ &- r_1\sin(2(t-\tau_3)))Z_2(t-\tau_3) \\ &+ \alpha\exp(-\rho\tau_3)(s_2\cos(t-\tau_3) \\ &- r_2\sin(t-\tau_3))\dot{Z}_1(t-\tau_3) \\ &- \left(2\rho + \frac{4\mu_2\omega_2}{\Omega}\right)\dot{Z}_2 \\ &+ 2\exp(-\rho\tau_3)\alpha(s_1\cos(2(t-\tau_3)) \\ &- r_1\sin(2(t-\tau_3)))\dot{Z}_2(t-\tau_3). \qquad (45)\end{aligned}$$

The first order approximate solutions of Eqs. (44) and (45) can be expressed as

$$\begin{aligned}Z_1(t) &= p_0 + p_1\cos t + p_2\sin t \\ &\quad + p_3\cos 2t + p_4\sin 2t, \qquad (46) \\ Z_2(t) &= p_5 + p_6\cos t + p_7\sin t.\end{aligned}$$

Inserting (46) into (44), (45) and equating the coefficients of same harmonic terms yield a set of linear homogeneous algebraic equations governing the coefficients p_0, p_1, p_2, p_3, p_4, p_5, p_6, p_7. Since the eight coefficients are not all zero, the determinant of the coefficients matrix, which is the so-called Hill's determinant, must be zero. Expanding this determinant yields

$$\begin{aligned}&\rho^{16} + f_1\left(\exp\left(-\frac{1}{2}\Omega\rho\tau_1\right), \exp\left(-\frac{1}{2}\Omega\rho\tau_2\right),\right. \\ &\left.\exp\left(-\frac{1}{2}\Omega\rho\tau_3\right)\right)\rho^{15} \\ &\quad + \cdots + f_{15}\left(\exp\left(-\frac{1}{2}\Omega\rho\tau_1\right), \exp\left(-\frac{1}{2}\Omega\rho\tau_2\right),\right. \\ &\left.\exp\left(-\frac{1}{2}\Omega\rho\tau_3\right)\right)\rho \\ &\quad + f_{16} = 0. \qquad (47)\end{aligned}$$

Since Eq. (47) has many exponential type transcendental terms, numerical methods are resorted to solve this equation. If the real parts of all characteristic exponents are negative, the periodic solution is asymptotically stable. On the other hand, if the real part of at least one characteristic exponent is positive, the periodic solution is unstable.

6 Quadratic position feedback and quadratic velocity feedback

In this section, the performance of the Feedback (1) control and the Feedback (2) control are compared. From the amplitude equations (36) and (39), we conclude that: if Feedback (1) is utilized, the amplitude of the primary system is $A_1 = \frac{\mu_2\omega_1^2}{|\alpha|}$ when $\sigma_1 = \sigma_2 = 0$; if Feedback (2) is utilized, the amplitude of the primary system is $A_1 = \frac{2\mu_2}{|\alpha|}$ when $\sigma_1 = \sigma_2 = 0$. It follows that: if $\omega_1^2 > 2$, the vibration reduction effect of Feedback (2) is better than that of Feedback (1), but not vice versa.

In the following sections, the parameters are fixed at $\mu_1 = 0.01$, $\alpha_1 = 14.41$, $\beta = 0.93$, $\gamma = 0.01$, $\mu_2 = 0.0001$, $\alpha = 0.7$, $f = 0.05$, $\omega_1 = 3.06$, unless otherwise specified.

Figure 1 shows the frequency–response curves of the primary system and the controller when $\sigma_2 = 0$. It can be seen that the effective frequency bandwidth of Feedback (2) is wider than that of Feedback (1) and the frequency–response curve of Feedback (2) is lower than that of Feedback (1) under the saturation control. It means that the vibration reduction effect of Feedback (2) is better than that of Feedback (1). However, the controller has the high-amplitude response under the Feedback (2) control when the excitation frequency is far from the resonance point (i.e., $\sigma_1 = 0$). It follows that the overload risk of the controller under Feedback (2) control is greater than that under Feedback (1) control. In the following, our efforts are focused on the Feedback(2) controlled system.

7 Effects of the control parameters

In this section, we divide three cases, i.e., $\sigma_2 = 0$; $\sigma_1 + \sigma_2 = 0$; $\sigma_1 = 0$ to discuss the effects of the control parameters $\alpha, \gamma, \mu_2, \lambda, \tau_1, \tau_2, \tau_3$ on the behavior of the Feedback (2) controlled system.

(1) Effect of the feedback gain α

Figure 2a1, a2 and a3 illustrates that increasing α can broaden the effective frequency bandwidth of the saturation controller and enhance the vibration reduction effect of the primary system. From Fig. 2b1, b3, we observe that the overload risk of the controller increases as the feedback gain α increases. Figure 2b2 shows that the saturation controller in the case $\sigma_1 + \sigma_2 = 0$ has the widest effective frequency bandwidth comparing with the two cases $\sigma_2 = 0$ and $\sigma_1 = 0$.

(2) Effect of the feedback gain γ

From the amplitude equation (36), we observe that the amplitude of the primary system is independent of the feedback gain γ. Therefore, the variation of γ does not affect the amplitude of the primary system. Figure 3 shows that increasing γ does not affect the effective frequency bandwidth of the saturation controller, but it can suppress the vibration of the controller. So, the feedback gain γ can be used as an important parameter to avoid the controller overload risk.

(3) Effect of the feedback gain λ

Figure 4b1, b3 shows that increasing λ can shrink the effective frequency bandwidth of the saturation controller for the two cases $\sigma_2 = 0$ and $\sigma_1 = 0$. Figure 4b2 shows that increasing λ has little effect on the effective frequency bandwidth of the saturation controller for the case $\sigma_1 + \sigma_2$. From Fig. 4 a1, a2, a3, we observe that increasing λ can suppress the vibration of the primary system when the saturation controller does not activate.

(4) Effect of the damping coefficient μ_2

Figure 5 shows that the smaller controller damping ratio, the wider effective frequency bandwidth of the

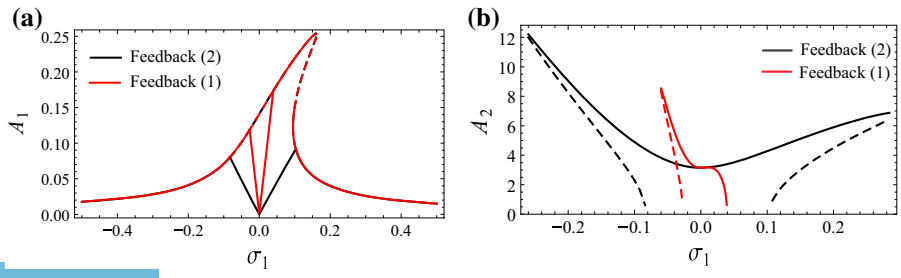

Fig. 1 Frequency–response curves of the saturation controlled system when $\sigma_2 = 0$, the solid line for stable solutions and the *dashed line* for unstable solutions. **a** the primary system; **b** the controller

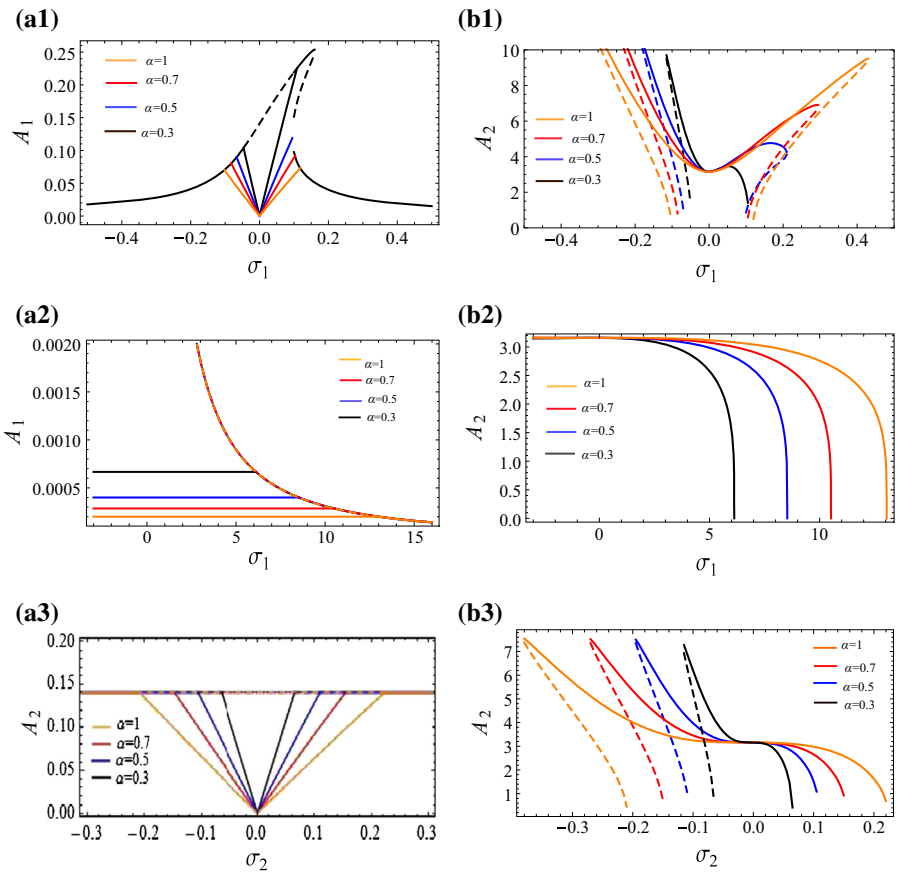

Fig. 2 Effect of varying α on the frequency–response curves: **a1**, **b1** $\sigma_2 = 0$; **a2**, **b2** $\sigma_1 + \sigma_2 = 0$; **a3**, **b3** $\sigma_1 = 0$

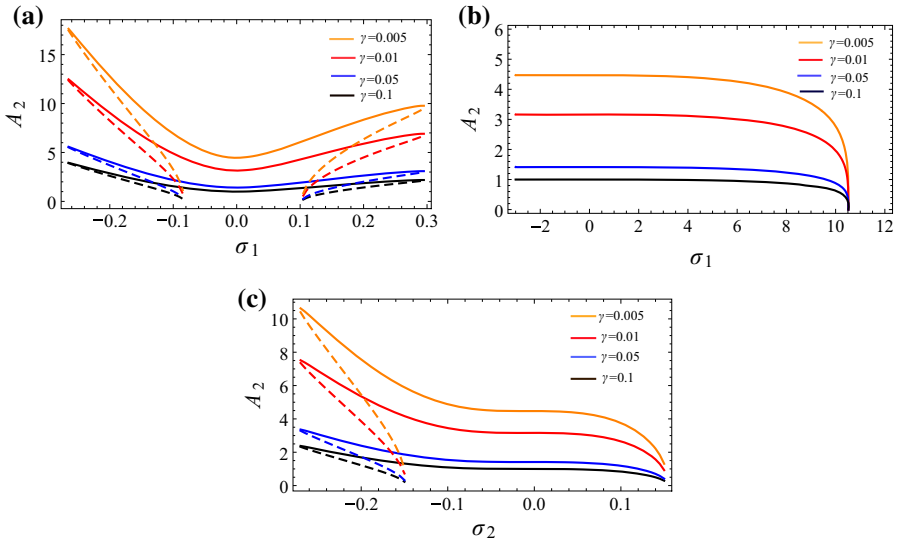

Fig. 3 Effect of varying γ on the frequency–response curves: **a** $\sigma_2 = 0$; **b** $\sigma_1 + \sigma_2 = 0$; **c** $\sigma_1 = 0$

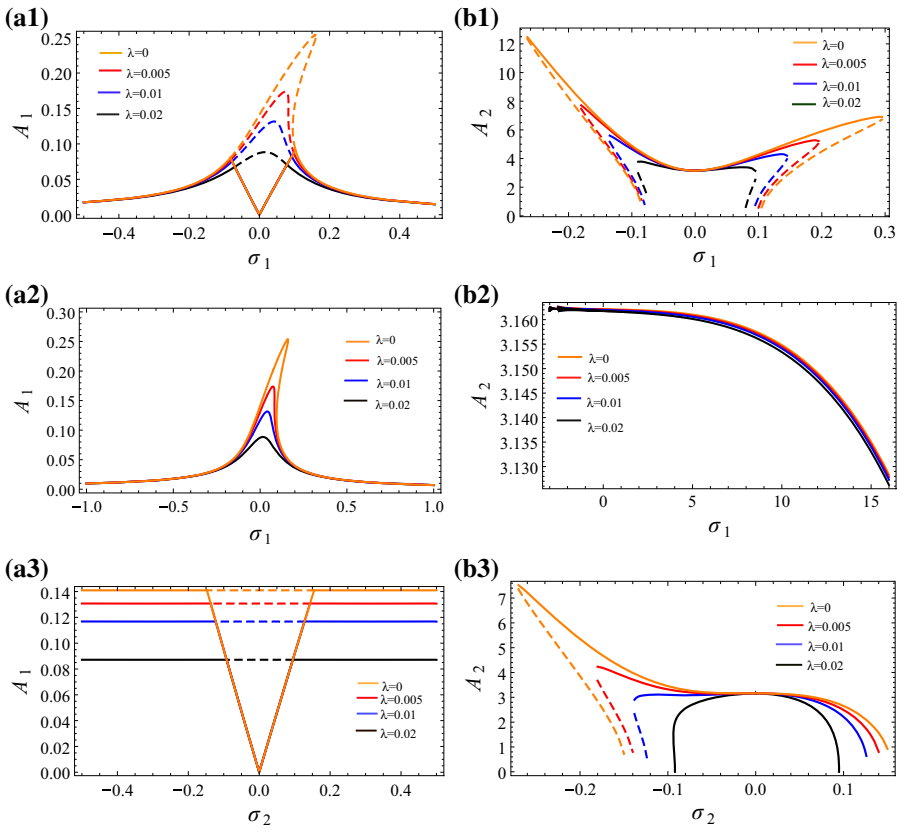

Fig. 4 Effect of varying λ on the frequency–response curves of the controller: **a1**, **b1** $\sigma_2 = 0$; **a2**, **b2** $\sigma_1 + \sigma_2 = 0$; **a3**, **b3** $\sigma_1 = 0$

controller and the better vibration reduction effect of the primary system. We also observe that the amplitude of the controller increases as μ_2 decreases. So, the smaller the μ_2, the bigger the overload risk of the saturation controller.

(5) Effect of time delay τ_2

From the amplitude equation (36), we observe that the amplitude of the primary system is independent of time delay τ_2. Figure 6 shows the amplitude (A_2)-delay (τ_2) response curves of the controller when $\sigma_1 = \sigma_2 = 0$, $\lambda = 0$. It can be seen that the amplitude (A_2)-delay (τ_2) response curve is stable in the delay interval [0, 0.12] and [1.88, 2.23]. Away from this range, the saturation controlled system becomes unstable. The appearance of time delay τ_2 can shrink the effective frequency bandwidth and suppress the vibration of the saturation controller as shown in Fig. 7a, c. So, time delay τ_2 can be used as an important parameter to avoid the controller overload risk. Figure 7b shows that time delay τ_2 has little effect around $\sigma_1 = 0$, and the saturation controlled system may lose stability at some values of time delay τ_2 for the case $\sigma_1 + \sigma_2$. So, time delay τ_2 should be tuned to zero for this case.

(6) Effect of time delay τ_3

The effect of time delay τ_3 is similar to that of τ_2. From the amplitude equation (36), it can be observed that the amplitude of the primary system is independent of time delay τ_3. Figure 8 shows that time delay τ_3 should be chosen in the interval [0,0.2]. For other range of τ_3, the saturation controlled system becomes unstable. Although the appearance of time delay τ_3 can shrink the effective frequency bandwidth of the saturation controller, it can suppress the vibration of the controller as shown in Fig. 9a, c. So, the time delay τ_3 can also be used as an important parameter to avoid the controller overload risk. However, for the case $\sigma_1 + \sigma_2 = 0$, the saturation controlled system loses stability near $\sigma_1 = 0$ and time delay τ_3 has little effect as shown in Fig. 9b. Therefore, it is important to tune time delay τ_3 to zero for this case.

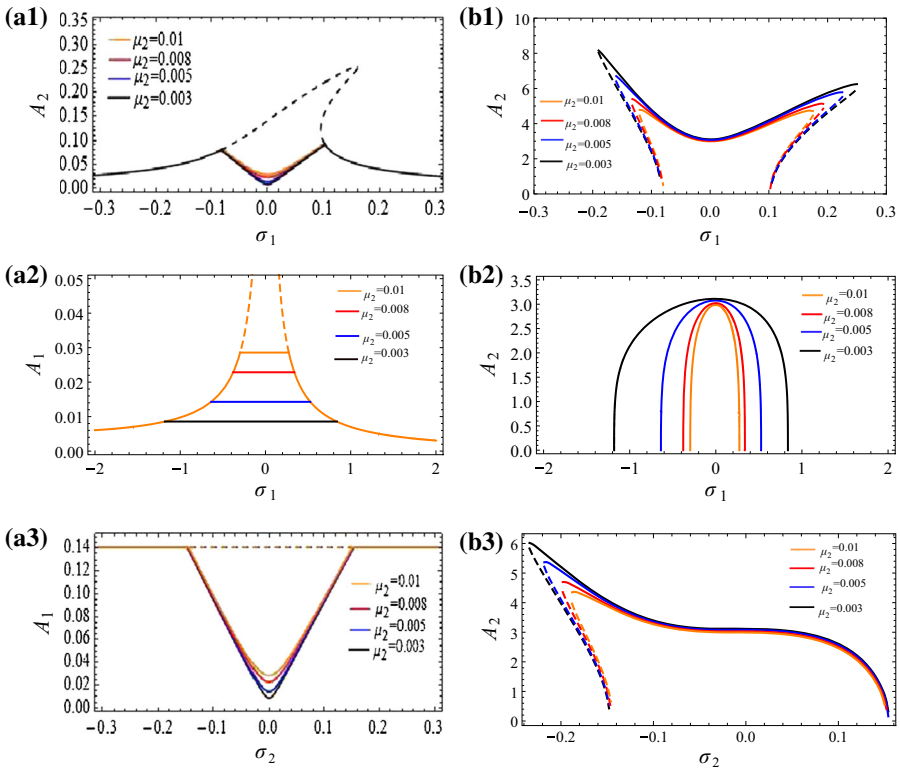

Fig. 5 Effect of varying μ_2 on the frequency–response curves: **a1**, **b1** $\sigma_2 = 0$; **a2**, **b2** $\sigma_1 + \sigma_2 = 0$; **a3**, **b3** $\sigma_1 = 0$

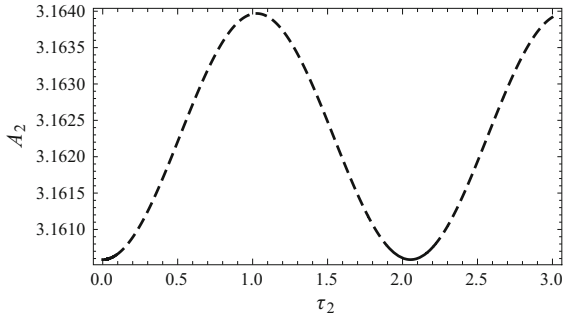

Fig. 6 Amplitude A_2-delay τ_2 response curve when $\sigma_1 = \sigma_2 = 0$, $\tau_1 = \tau_3 = 0$

(7) Effect of time delay τ_1

For $\sigma_1 = \sigma_2 = 0$, $\lambda = 0.01$, the amplitude (A_2)-delay (τ_1) curve has three stable segments: [0, 0.7], [1.35, 2.8] and [3.4, 4.85] as shown in Fig. 10. Away from these ranges, the saturation controlled system lose stabilities. For the case $\sigma_2 = 0$, proper choice of time delay τ_1 can broaden the effective frequency bandwidth as shown in Fig. 11a1, b1. From Fig.11a3, b3, we observe that the appearance of τ_1 can shrink the effective frequency bandwidth for the case $\sigma_1 = 0$. Figure 11a2, b2 shows that time delay τ_1 has little effect on the case $\sigma_1 + \sigma_2 = 0$.

8 Numerical simulations

First, the approximate results obtained by the integral iterative method are compared with numerical simulations quantitatively. Figure 12 shows a comparison of frequency–response curves obtained by the integral iterative method and numerical simulations when $\sigma_2 = 0$, $\lambda = 0$, $\tau_1 = 0$, $\tau_2 = 0$, $\tau_3 = 0$. Figure 13 shows a comparison between the approximate solutions and numerical solutions for force-response curves when $\sigma_1 = 0$, $\sigma_2 = 0$, $\mu_2 = 0.01$, $\lambda = 0.01$, $\tau_1 = 0.1$, $\tau_2 = 0.05$, $\tau_3 = 0.1$. As shown in these figures, the approximate solutions are in good agreement with numerical simulations, which indicates that the above analysis is valid.

Figure 14 shows time histories of the primary system and the controller for three different cases, i.e., uncontrol, Feedback (1) control and Feedback (2) control. From Fig. 14a, it is observed that the amplitude of the

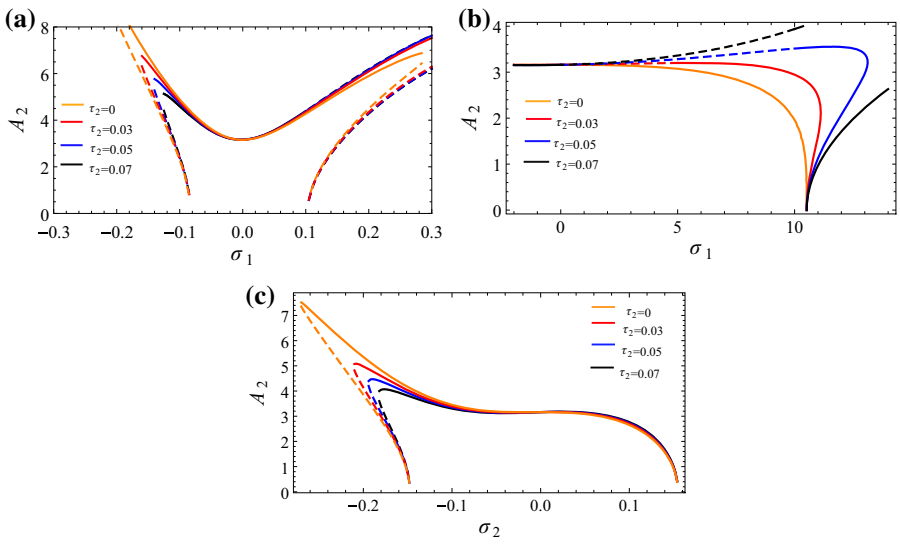

Fig. 7 Effect of varying τ_2 on the frequency–response curves of the controller: **a** $\sigma_2 = 0$; **b** $\sigma_1 + \sigma_2 = 0$; **c** $\sigma_1 = 0$

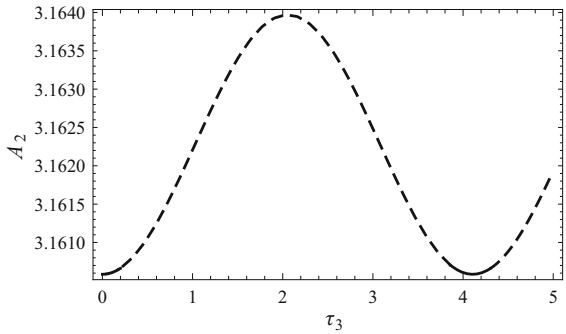

Fig. 8 Amplitude A_2-delay τ_3 response curve when $\sigma_1 = \sigma_2 = 0$, $\tau_1 = \tau_2 = 0$

primary system under Feedback (2) control is almost zero and smaller than that under Feedback (1) control. Figure 14b shows that the amplitudes of the controller under two different control is almost the same.

Figures 15 and 16 show time histories of the primary system and the controller for $\gamma = 0.01$ and $\gamma = 0.1$, respectively, where $\alpha = 1$, $\sigma_1 = -0.28$, $\sigma_2 = 0$. It can be seen that the controller steady-state amplitude is about 10 when $\alpha = 1$, $\gamma = 0.01$, $\sigma = -0.28$, $\sigma_2 = 0$. As γ increases to 0.1, the amplitude of the controller decreases to about 3. These figures show that increasing

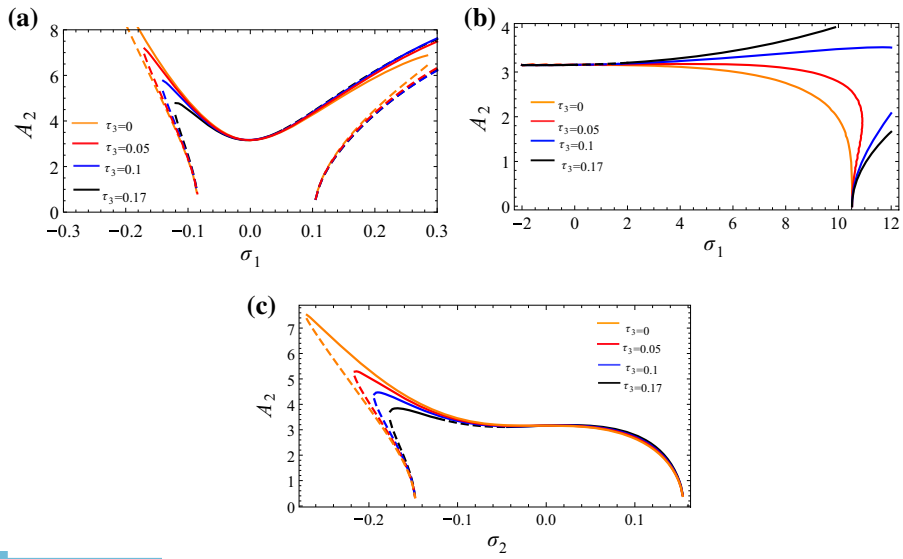

Fig. 9 Effect of varying τ_3 on the frequency–response curves of the controller: **a** $\sigma_2 = 0$; **b** $\sigma_1 + \sigma_2 = 0$; **c** $\sigma_1 = 0$

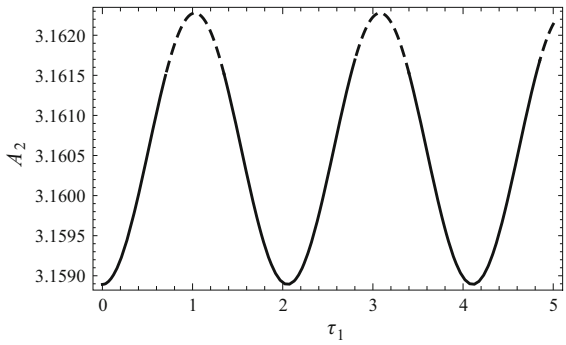

Fig. 10 Amplitude A_2-delay τ_1 response curve when $\sigma_1 = \sigma_2 = 0,\ \tau_2 = \tau_3 = 0$

the feedback gain γ suppresses the steady-state vibration of the controller.

Figures 17 and 18 show time histories of the primary system and the controller for $\lambda = 0$ and $\lambda = 0.05$ respectively, where $\sigma_1 = \sigma_2 = 0,\ \tau_1 = 0$. Figures 19 and 20 show time histories of the primary system and the controller for $\lambda = 0$ and $\lambda = 0.1$ respectively, where $\sigma_1 = -0.5,\ \sigma_2 = 0.5,\ \tau_1 = 0$. To ensure that the saturation controller activates, the initial conditions are takes as $u(0) = 0.5, v(0) = 4, \dot{u}(0) = -1, \dot{v}(0) = 1$ in these figures. Comparing Figs. 17 and 18, we observe that the transient times to reach the steady-state vibrations decrease greatly because of proper choice of

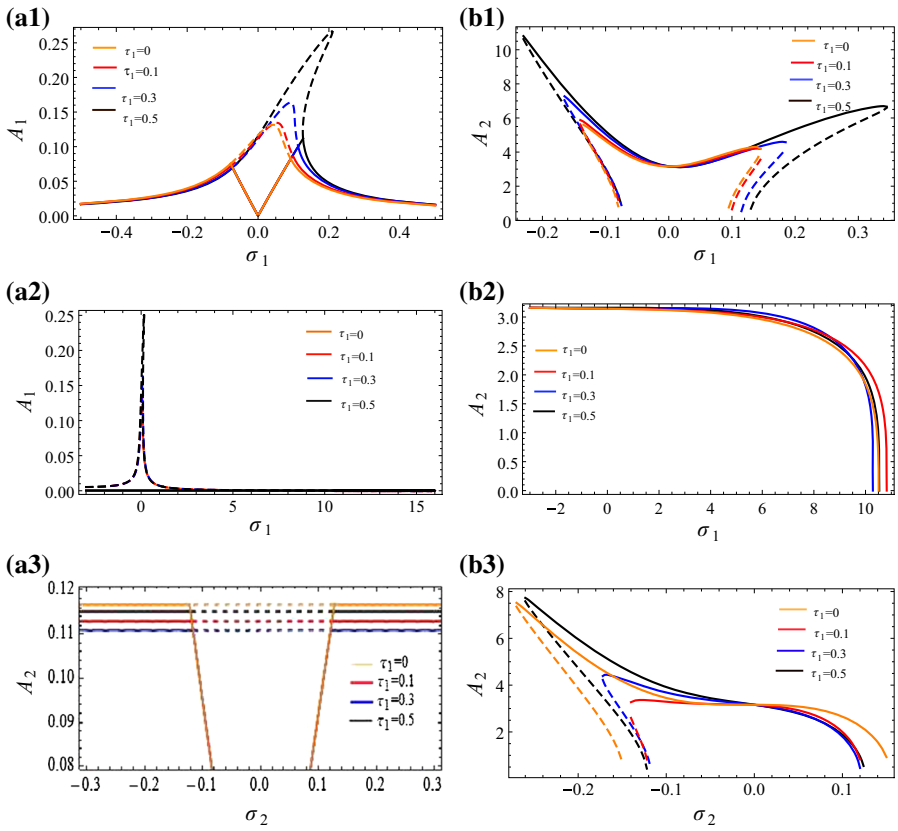

Fig. 11 Effect of varying τ_1 on the frequency–response curves: **a1**, **b1** $\sigma_2 = 0$; **a2**, **b2** $\sigma_1 + \sigma_2 = 0$; **a3**, **b3** $\sigma_1 = 0$

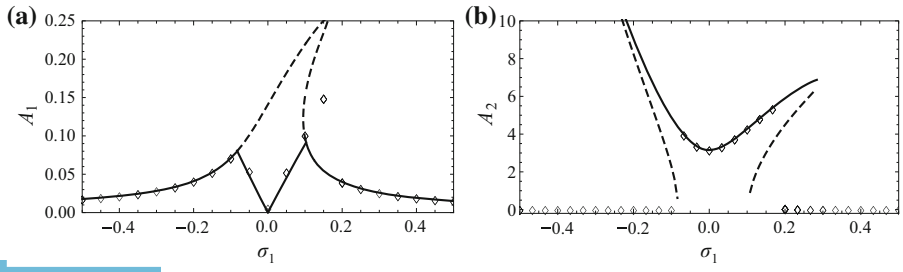

Fig. 12 Comparison of frequency–response curves between numerical solutions and approximate solutions obtained by the integral iterative method when $\sigma_2 = 0, \lambda = 0,\ \tau_1 = 0,\ \tau_2 = 0,\ \tau_3 = 0$, **a** the primary system; **b** the controller

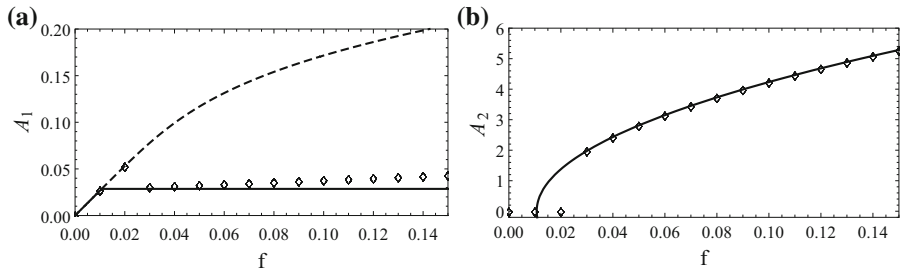

Fig. 13 Comparison of force-response curves between numerical solutions and analytical solutions obtained by the integral iterative method when $\sigma_1 = 0,\ \sigma_2 = 0,\ \mu_2 = 0.01,\ \lambda = 0.01,\ \tau_1 = 0.1,\ \tau_2 = 0.05,\ \tau_3 = 0.1$, **a** the primary system; **b** the controller

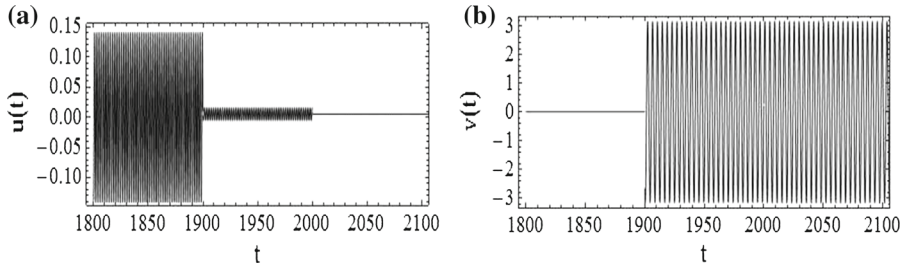

Fig. 14 Time histories of the primary system and the controller when $\sigma_1 = \sigma_2 = 0,\ \lambda = 0,\ 1800 \le t \le 1900$, uncontrol; $1900 \le t \le 2000$, Feedback (1) control; $2000 \le t \le 2100$, Feedback (2) control

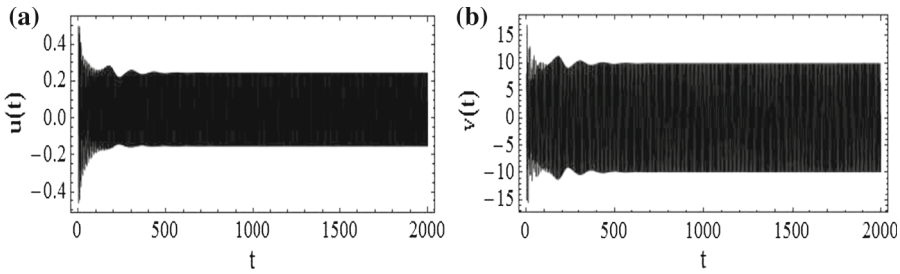

Fig. 15 Time histories of the primary system and the controller when $\alpha = 1,\ \gamma = 0.01,\ \sigma_1 = -0.28,\ \sigma_2 = 0$, initial condition: $u(0) = 0.5,\ v(0) = 8,\ \dot{u}(0) = -1,\ \dot{v}(0) = 1$

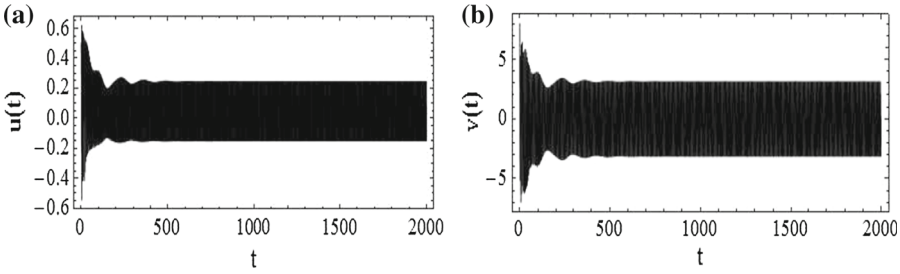

Fig. 16 Time histories of the primary system and the controller when $\alpha = 1,\ \gamma = 0.1,\ \sigma_1 = -0.28,\ \sigma_2 = 0$, initial condition: $u(0) = 0.5,\ v(0) = 8,\ \dot{u}(0) = -1,\ \dot{v}(0) = 1$

λ. The same phenomenon can be observed by comparing Figs. 19 and 20. However, Figs. 17 and 19 show that the transient times required increase as the detuning values $\sigma_1,\ \sigma_2$ increase. Combining these figures, it can be concluded that proper choice of λ can effectively suppress the transient vibrations.

9 Conclusion

To control the transient and steady-state vibrations of a nonlinear composite beam, an improved time-delayed saturation controller is proposed by using quadratic time-delay velocity coupling term instead of the orig-

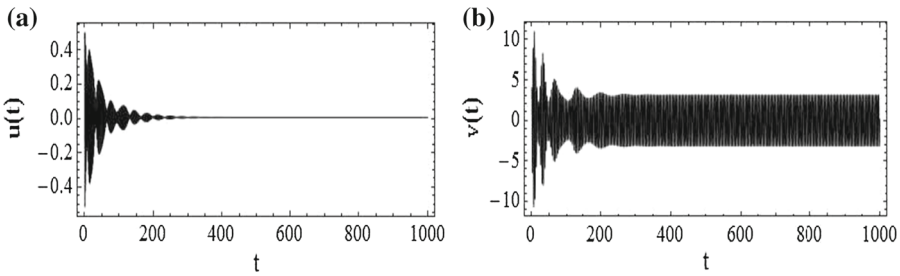

Fig. 17 Time histories of the primary system and the controller when $\lambda = 0,\ \sigma_1 = \sigma_2 = 0$ initial condition: $u(0) = 0.5,\ v(0) = 4,\ \dot{u}(0) = -1,\ \dot{v}(0) = 1$

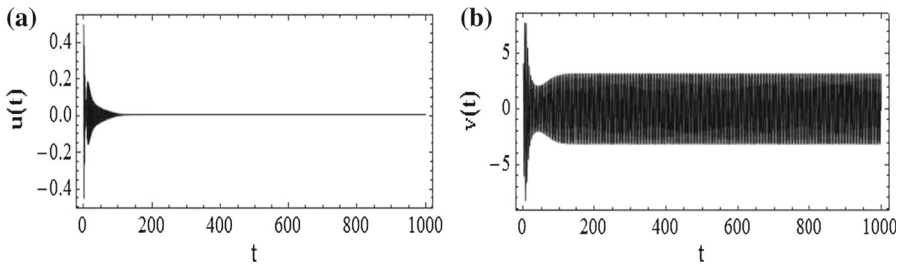

Fig. 18 Time histories of the primary system and the controller when $\lambda = 0.05,\ \sigma_1 = \sigma_2 = 0,\ \tau_1 = 0$, initial condition: $u(0) = 0.5,\ v(0) = 4,\ \dot{u}(0) = -1,\ \dot{v}(0) = 1$

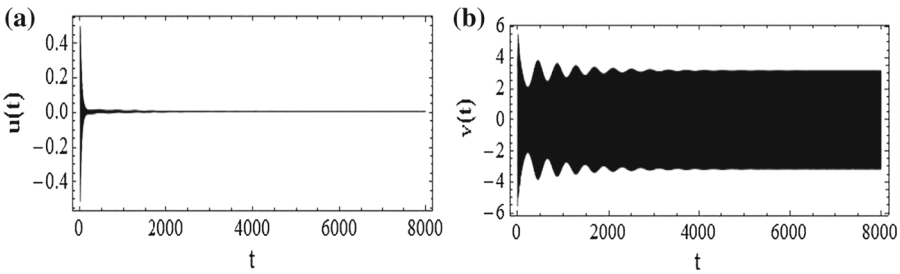

Fig. 19 Time histories of the primary system and the controller when $\lambda = 0,\ \sigma_1 = -0.5,\ \sigma_2 = 0.5,\ \tau_1 = 0$, initial condition: $u(0) = 0.5,\ v(0) = 4,\ \dot{u}(0) = -1,\ \dot{v}(0) = 1$

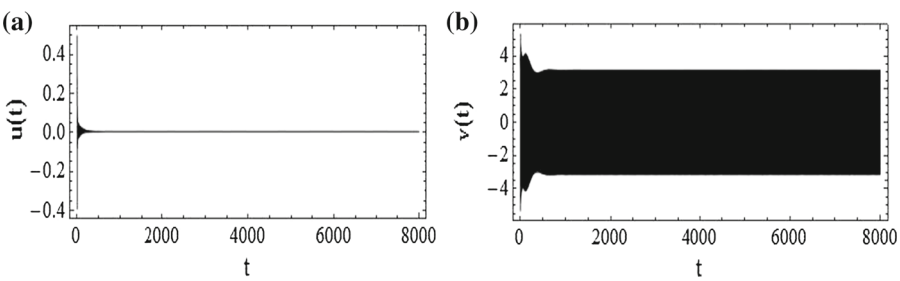

Fig. 20 Time histories of the primary system and the controller when $\lambda = 0.1,\ \sigma_1 = -0.5,\ \sigma_2 = 0.5,\ \tau_1 = 0$, initial condition: $u(0) = 0.5,\ v(0) = 4,\ \dot{u}(0) = -1,\ \dot{v}(0) = 1$

inal quadratic position coupling term in the controller and adding a negative time-delay velocity feedback to the primary system. A new analytical method named the integral iterative method is utilized to derive the second-order approximations and the amplitude equations when the primary resonance and 1:2 internal resonance occur simultaneously. Then, the stability of the periodic solution is investigated using the Floquet theory. From the above analysis, the main results are summarized as follows.

(1) The analytical predictions based on the integral iterative method is in good agreement with numerical simulations both quantitatively and qualitatively.
(2) The quadratic velocity coupling term can enlarge the effective frequency bandwidth and enhance the performance of the vibration reduction by comparison with the original quadratic position coupling term. In addition, the linear velocity feedback can effectively decreases the transient times.
(3) The performance of the improved saturation controller can be enhanced by properly adjusting the control parameters $\alpha, \gamma, \lambda, \mu_2, \tau_1, \tau_2, \tau_3$. Increas-

ing α or decreasingμ_2 can broaden the effective frequency bandwidth of the saturation controller, but increase its overload risk. However, increasing γ and proper choices of τ_1, τ_2, τ_3 can avoid the occurrence of the controller overload.

(4) Proper choice of time delay τ_1 can enlarge the effective frequency bandwidth of the saturation controller.

(5) Similar to the previous work [6], the saturation controller should be designed for two different cases. First, if the natural frequency of the primary system is easily changed and the excitation has a single frequency, device should be designed to trace the excitation frequency and keep the natural frequency of the controller equal to half of the excitation frequency in the control process. In this case, the saturation controller possess a wide effective frequency bandwidth. Second, if the natural frequency of the primary system is not easily changed, we should keep the natural frequency of the controller equal to one half of the natural frequency of the primary system.

10 Comparison with previously published work

In Ref.[20], Warminski selected four different controllers including nonlinear saturation controller (NSC) to suppress the nonlinear composite beam vibration and found that the PPF and NSC controllers are most effective. Based on the model in [20], Saeed [16] et al studied the effects of time delays on the saturation control. They found that time delays in the saturation controlled system can change the controller's frequency bandwidth and can avoid the occurrence of the controller overload. However, the coupling term in the controller is of quadratic position. In other words, the system in the previous two works [16,20] is under the Feedback (1) control. In [6], the authors proposed a refined vibration absorber that applied to a linear beam model. They found that the quadratic velocity coupling term enables the saturation controller to suppress the vibration of the primary system to zero, but the quadratic position coupling term cannot, and a negative velocity feedback can suppress the transient vibrations. So, in this paper we improved the NSC controllers in [16,20] by using quadratic velocity coupling term in the controller with time delay and adding a negative time-delay velocity feedback to the primary system. We found that the quadratic velocity coupling term can enlarge the effective frequency bandwidth and enhance the performance of the vibration by comparison with the original quadratic velocity coupling term in [16,20].

Acknowledgments This work is supported by the State Key Program of National Natural Science Foundation of China under Grant No.11032009, National Natural Science Foundation of China under Grant No.11272236 and the Strategic Research Grant No.7004242 of the City University of Hong Kong.

References

1. Nayfeh, A.H., Mook, D.T., Marshall, L.R.: Non-linear coupling of pitch and roll modes in ship motion. J. Hydronaut. **7**, 145–152 (1973)
2. Haddow, A.G., Barr, A.D.S., Mook, D.T.: Theoretical and experimental study of modal interaction in a two-degree-of-freedom structure. J. Sound Vib. **97**, 451–473 (1984)
3. Oueini, S.S., Nayfeh, A.H., Golnaraghi, M.F.: A theoretical and experimental implementation of a control method based on saturation. Nonlinear Dyn. **13**, 189–202 (1997)
4. Oueini, S.S., Nayfeh, A.H., Pratt, J.R.: A nonlinear vibration absorber for flexible structures. Nonlinear Dyn. **15**, 259–282 (1998)
5. Oueini, S.S., Nayfeh, A.H.: Analysis and application of a nonlinear vibration absorber. J. Vib. Control. **6**, 999–1016 (2000)
6. Pai, P.F., Schulz, M.J.: A refined nonlinear vibration absorber. Int. J. Mech. Sci. **42**, 537–560 (2000)
7. Xu, J., Chung, K.W., Zhao, Y.Y.: Delayed saturation controller for vibration suppression in stainless-steel beam. Nonlinear Dyn. **62**, 177–193 (2010)
8. Li, J., Hua, H.X., Shen, R.Y.: Saturation-based active absorber for a non-linear plant to a principal external excitation. Mech. Syst. Signal Process. **21**, 1489–1498 (2007)
9. El-Badawy, A.A., El-Deen, T.N.N.: Quadratic nonlinear control of a self-excited oscillator. J. Vib. Control. **13**, 403–414 (2007)
10. Li, J., Li, X.B., Hua, H.X.: Active nonlinear saturation-based control for suppressing the free vibration of a self-excited plant. Commun. Nonlinear Sci. Numer. Simul. **15**, 1071–1079 (2010)
11. Sayed, M., Kamel, M.: 1:2 and 1:3 internal resonance active absorber for non-linear vibrating system. Appl. Math. Model. **36**, 310–332 (2012)
12. Warminski, J., Cartmell, M.P., Mitura, A., et al.: Active vibration control of a nonlinear beam with self-and external excitations. Shock Vib. **20**, 1033–1047 (2013)
13. Kamel, M., Kandil, A., El-Ganaini, W.A., et al.: Active vibration control of a nonlinear magnetic levitation system via nonlinear saturation controller (NSC). Nonlinear Dyn. **77**, 605–619 (2014)
14. Long, F.: Time-delay induced symmetry restoration and noise enhanced stability phenomena under correlated noises in an asymmetric bistable system. Indian J. Phys. **88**, 1111–1116 (2014)

15. Zhao, Y.Y., Xu, J.: Using the delayed feedback control and saturation control to suppress the vibration of dynamical system. Nonlinear Dyn. **67**, 735–753 (2012)
16. Saeed, N.A., El-Ganini, W.A., Eissa, M.: Nonlinear time delay saturation-based controller for suppression of nonlinear beam vibrations. Appl. Math. Model. **37**, 8846–8864 (2013)
17. He, W., Ge, S.S., How, B.V.E., et al.: Robust adaptive boundary control of a flexible marine riser with vessel dynamics. Automatica **47**, 722–732 (2011)
18. He, W., Zhang, S., Ge, S.S.: Robust adaptive control of a thruster assisted position mooring system. Automatica **50**, 1843–1851 (2014)
19. He, W., Sun, C., Ge, S.S.: Top tension control of a flexible marine riser by using integral-barrier lyapunov function. IEEE/ASME Trans. Mech. **20**, 497–505 (2015)
20. Warminski, J., Bochenski, M., Jarzyna, W., Filipek, P., Augustyniak, M.: Active suppression of nonlinear composite beam vibrations by selected control algorithms. Commun. Nonlinear Sci. Numer. Simul. **16**, 2237–2248 (2011)
21. El-Ganaini, W.A., Saeed, N.A., Eissa, M.: Positive position feedback (PPF) controller for suppression of nonlinear system vibration. Nonlinear Dyn. **72**, 517–537 (2013)
22. Schmidt, G., Tondl, A.: Nonlinear Vibrations. Cambridge University Press, Cambridge (1986)
23. Chen, Y.L., Xu, J.: Applications of the integral equation method to delay differential equations. Nonlinear Dyn. **73**, 2241–2260 (2013)
24. Chen, Y.L., Chung, K.W., Xu, J., Sun, Y.X.: Analysis of vibration suppression of master structure in nonlinear systems using nonlinear delayed absorber. Int. J. Dyn. Control. **2**, 55–67 (2014)